Supporting Information

Sorre et al. 10.1073/pnas.1103594108

SI Text

Giant Unilamellar Vesicles (GUVs) Preparation. ***Reagents.*** Lipids 1,2-dioleoyl-sn-glycero-3-phosphocholine (DOPC), DSPE (di-stearoyl phosphatidyl ethanolamine)-PEG(2000)-Biotin, dioleylphosphatidylserine (DOPS), and dioleylphosphatidylethanolamine (DOPE) were purchased from Avanti Polar Lipids. BODIPY-FLC5-hexadecanoyl phosphatidylcholine (HPC*) and BODIPY-TR-C5-ceramide (Cer*) were obtained from Molecular Probes.

Electroformation technique. All the data presented in this study have been obtained with GUVs having the same lipid compositon : DOPC:DOPE:DOPS (1:1:1) + 0.03% DSPE-PEG(2000)-Biotin and 0.5% BODIPY TR ceramide. To obtain good yields with this composition containing a high amount of negatively charged lipids, we had to adapt the original electroformation protocol described in refs. 1 and 2. Ten microliters of lipid mix at 0.5 mg/mL were deposited on conductive indium-tin oxide (ITO) coated glass (Präzisions Glas and Optik), The lipid film was dried for a few minutes at 60 °C to obtain better homogeneity in the lipid film (3) and subsequently dried under high vacuum for at least 1 h. The lipid film was then rehydrated in a sucrose solution (osmolarity 100–300 mOsm) in a growth chamber made of two ITO electrodes separated by 1 mm. We observed that charged vesicles grew much faster than those with zwitterionic lipids. As a consequence, only 30 min of growth under a sinusoidal voltage of 850 mV rms amplitude and 10 Hz frequency were sufficient to obtain a large number of vesicles.

Protein Purifications. Human amphiphysin 1 was purified using the standard GST fusion expression protocol as detailed in the manufacturer literature (Glutathione Sepharose 4B from GE Healthcare). Bacteria (BL21 *Escherichia coli*) were transfected with a plasmid expressing GST fusion of the proteins of interest under the control of an IPTG sensitive inducer, a generous gift from P. de Camilli (Yale, New Haven, CT). Protein production was induced by addition of 1 mM IPTG in the culture medium during 3 h at 37 °C or overnight at 30 °C. GST fusion amphiphysin 1 was purified from cell lysate using GST beads (GE Healthcare). The protein was eluted with 25 mM reduced glutathione in PBS at pH 7.8. GST was cleaved by GST-linked precision enzyme during overnight dialysis in experiment buffer (20 mM Hepes, 100 mM NaCl). The free GST and GST-linked precision enzyme were removed with another round of binding to GST beads. Amphiphysin 1 concentrations were measured using Bradford assay (Biorad) and light absorption at 280 nm (nanodrop). Our purification yielded 1 mL of 4.5 μM amphiphysin solution. An average number of three Alexa 488 bound was found per amphiphysin dimer, using extinction coefficient at 488 nm (nanodrop). Tubulating activity of the protein was checked using the flat membrane sheets tubulation assay (4).

Experimental Protocol for Tube Pulling Experiments. In order to study the impact of a soluble membrane-deforming protein on membrane mechanical properties, the tube pulling protocol that we have used in our previous studies (5, 6) had to be slightly modified: Fluorescent Alexa 488-labeled amphiphysin 1 (amph1*) was not present in bulk in the experiment chamber. Instead, it was injected near the GUV under study, using the microinjection protocol presented in the following.

Microinjection was chosen for three reasons: (*i*) This protocol permits us to reach high local amph1* concentration while using only a small amount of protein. (*ii*) When amph1* is present everywhere in solution prior to micromanipulation, GUV are often found to be already tubulated (see Fig. 1*C*), which is not compatible with tube pulling experiments. Microinjection allows us to control the initiation of amph1* binding. (*iii*) Finally, before injection of amph1*, the mechanical characteristics of each GUV in the absence of amph1* can be measured, providing a reference for each experiment. We used large pipettes (about 10 μm in diameter). To control the injection pressure, we used a hydrostatic system similar to the one we used to control the membrane tension (see *Materials and Methods* in text). The pipette was first filled by the tip to prevent jamming with a few microliters of protein solution and then backfilled with mineral oil. Oil prevented diffusion of our protein into the water of the pressure control system. A pressure as low as 10 Pa was sufficient to inject protein only around the vesicle under study, with flow speed low enough to avoid force measurement perturbation. This protocol allowed us to monitor in real time the effects of protein binding on membrane mechanical properties.

A typical experiment went as follows. A GUV, made of DOPC:DOPE:DOPS (1:1:1), initially under low membrane tension (showing optically visible fluctuations) was grabbed with the aspiration pipette. A tube was pulled with an optically trapped bead, and the membrane tension (σ) was increased step by step by rising micropipette aspiration. For each membrane tension, the force necessary to hold the tube was recorded. Once at high membrane tension, the injection pipette containing amph1* in solution was brought in the field of view, close to GUV (typically 10–20 μm). The injection flow was slow enough ($<\mu m \cdot s^{-1}$) not to perturb the force measurement and the osmolarity of the injection buffer was matched to the experiment buffer to avoid any osmotic shock during injection. The membrane tension was kept constant until the amph1* fluorescence signal on the GUV was stabilized (5–10 min). The membrane tension was then decreased step by step. The protein solution was continuously injected during the course of the experiment, keeping the bulk concentration constant near the GUV. At both low and high concentrations, we observed that amph1* binding to the tube was homogeneous along the length of the tube (Fig. S7), and took approximately 1 min to reach steady state. For each value of the tension, the force was recorded and an image was acquired. We checked that, when a buffer solution without protein was injected, the forward and backward curves were superimposed and that the force (f) was linear with $\sqrt{\sigma}$ (see Fig. S3). By fitting these curves, we obtained a value of the bending rigidity of $\kappa = 12 \pm 4\ k_BT$ for our DOPC:DOPE:DOPS mix.

Tube Radius Measurement. Our experimental setup provides two independent ways to measure the tube radius. The first method consists in using the well-established equilibrium relationship between the tube radius (R), the force necessary to hold the tube (f), and the membrane tension (σ) (7):

$$R = \frac{f}{4\pi\sigma}, \qquad \textbf{[S1]}$$

where f and σ are measured quantities in our system. This expression might not, however, be valid in cases where the membrane is covered by proteins.

We used a second, model-independent method to measure R that takes advantage of the fact that, in most experiments, the tube diameter is smaller than the thickness of the confocal

volume. The fluorescence signal coming from fluorescently labeled lipids in the membrane in the tube (I_t^l), normalized by the same intensity in the GUV (I_v^l), is proportional to the tube surface and thus to the tube radius. As a consequence, the fluorescence signal should be proportional to the radius value deduced from force and tension measurements:

$$R = F \times (I_t^l / I_v^l). \quad \textbf{[S2]}$$

The prefactor value ($F = 200 \pm 50$ nm, based on six independent measurements) has been calibrated experimentally using a linear fit of the radii values measured with force measurements in the absence of protein on the membrane, ($R = \frac{f}{4\pi\sigma}$) vs. I_t^l/I_v^l; see Fig. S4.

Measurement of Protein Density on the Membrane. The fluorescence signal measured using confocal microscopy is proportional to the number of fluorescent molecules in the confocal volume; it is therefore possible to transform the fluorescence values given by the microscope (in gray levels, arbitrary units) into a density of bound molecules per unit area, if an appropriate calibration method is used. We have adapted the "supported lipid bilayer standard" method proposed by ref. 8. The standard used is a lipid bilayer containing a controlled amount of a lipid dye emitting in the same channel as the labeled protein of interest. In ref. 8, the standard used is a flat supported bilayer because the object of their study has a flat geometry (adherent cells). Here, we used GUVs containing BodipyFL-C5-HPC (HPC*), a green fluorescent labeled lipid, at various concentrations. An image analysis procedure used to extract fluorescence values from images has been described elsewhere (5). We found that the measured fluorescent signal ($I_v^{\mathrm{HPC}^*}$) from GUV was linear with HPC* for area density $\Phi_v^{\mathrm{HPC}^*}$ up to 14,000 HPC* per μm^2 (*ca.* 0.5 mol %); see Fig. S1*A*:

$$\Phi_v^{\mathrm{HPC}^*} = A^{\mathrm{gain}} \times I_v^{\mathrm{HPC}^*}. \quad \textbf{[S3]}$$

The conversion constant A^{gain} was measured for various gains of the confocal photomultiplier tube detector (PMT). For the example presented in Fig. S1*A* (PMT gain = 110), we found $A^{110} = 3.80 \pm 0.15$ (based on two independent measurements). Eq. **S3** is however only valid to quantify HPC* fluorescence in the membrane. Because amph1* will have a different efficiency than HPC*, the calibration must be corrected to take into account the spectral differences of the two fluorophores and how those spectra are affected by the microscope optics:

$$\Phi_v = \frac{A^{\mathrm{gain}} \times I_v^a}{F_1}, \quad \textbf{[S4]}$$

where $F_1 = I_{\mathrm{bulk}}^a / I_{\mathrm{bulk}}^{\mathrm{HPC}^*}$ is the ratio of fluorescence intensities of amph1* and HPC*, respectively, at a given concentration in solution, and I_v^a is the fluorescence signal coming from amph1* measured on the GUV. F_1 is deduced from the evolution of the intensity ratio measured in solution, as a function of the concentration of labeled molecules in bulk. In the case of HPC*, which is an insoluble molecule, we measured the bulk fluorescence of a solution of small unilamellar vesicles (SUVs) which have a size below optical resolution. We found that both signals of amph1* and HPC* in SUVs in bulk were linear with labeled molecule concentration (Fig. S1 *B* and *C*, respectively). F_1 is the ratio of the slope of the linear fits to graphs *C* and *B* in Fig. S1. Ultimately, we used a value of $F_1 = 1.8 \pm 0.1$, this value is independent on the PMT gains. Because there is an average of three Alexa 488 molecules on each amph1* dimer, corresponding to a relative efficiency of Alexa 488 to BodipyFL-HPC of 0.6, a value comparable to those found by Galush et al. (8). Finally, for a given value of PMT gain, the area density of amph1* on the GUV (Φ_v), in number of molecules bound per μm^2, is then

$$\Phi_v = \mathrm{cal} \times I_v^a, \quad \textbf{[S5]}$$

where $\mathrm{cal} = A^{\mathrm{gain}}/F_1$ is the conversion constant between fluorescence signal due to amph1* and its density on the membrane, for a given value of the PMT gain of the confocal.

We note that the relative error on protein density, Φ_v, is the sum of the relative error on the fluorescence calibration (10%, see above) and the relative error on the fluorescence measurements from a single GUV. In a single experiment, the amph1* fluorescence on the GUV is measured typically 5–10 times. The error on the fluorescence measurement is thus given by the standard deviation.

Amphiphysin density on the tube. Amphiphysin density on the tube Φ_t is given by

$$\Phi_t = S \times \Phi_v, \quad \textbf{[S6]}$$

where *S*, the sorting ratio, is defined as the relative enrichment of amphiphysin on the tube compared to the GUV: $S = \frac{I_t^a}{I_v^a} / \frac{I_t^l}{I_v^l}$, where I_t^a, I_t^l, and I_t^l are the fluorescence intensities per pixel of amph1* on the tube, of the lipid Cer* on the tube, and of Cer* on the GUV, respectively. It follows that the amphiphysin density on the tube is given by

$$\Phi_t = \frac{\mathrm{cal} \times I_v^l}{I_t^l} \times I_t^a. \quad \textbf{[S7]}$$

The lipid intensities are used here to eliminate geometric factors; we note that no sorting of Cer* occurs, as it is equally distributed on the tube and on the GUV.

Langmuir isotherm. The density of bound protein on the GUV follows a Langmuir binding isotherm (see Fig. 1*A*) when the amph1* bulk concentration is increased: $\Phi_v = \Phi_{\max}/[1 + (K_{\mathrm{d}}/C_{\mathrm{bulk}})]$. We found $K_{\mathrm{d}} = 35$ nM for the binding of amph1* on DOPC:DOPE:DOPS (1:1:1) GUVs. This value will change depending on the nature and the density of charged lipids in the membrane (9). This low K_{d} value reflects a strong asymmetry between binding and unbinding processes. Indeed, we have measured that for $C_{\mathrm{bulk}} \approx 1$ μM, it takes about 1 min to reach steady state when amph1* is injected, which corresponds to an on-rate $k_{\mathrm{on}} \approx 1/60$ μM^{-1} s^{-1}, and therefore an off-rate $k_{\mathrm{off}} = K_{\mathrm{d}} \cdot k_{\mathrm{on}} \approx 1/(30\ \mathrm{min})$. In fact, when a GUV is coated with amph1*, it takes more than 30 min (see Fig. S2) to desorb half of them, confirming the very slow desorption process. Our experiments are performed 2 or 3 min after injection, and usually last less than 10 min, implying that, in the high-concentration regime, the protein density on the GUV Φ_v is at steady state and constant during the measurement time, as confirmed experimentally. Moreover, as $\Phi_v \approx \Phi_{\max}$, we can consider that all DOPS molecules are saturated by proteins. In the second limiting regime corresponding to very low bulk concentrations, the time evolution of Φ_v is very slow, being proportional to $k_{\mathrm{on}} \cdot C_{\mathrm{bulk}} \approx 10^{-3}$ s^{-1} for $C_{\mathrm{bulk}} \approx$ 10 nM. Thus, the protein density on the membrane will be changed only by a factor 2 in 20 min.

Model of Amphiphysin Binding to Membrane Tubes. In this section, we present a theoretical model of the adsorption of amphiphysin to membrane tubes. In *Free energy* (below), we propose a free energy for a membrane tube connected to a vesicle. In *Protein binding in the dilute regime*, we consider the dilute regime and calculate the protein sorting, the tube radius, and the force

needed to hold the tube. In *Protein binding in the concentrated regime*, we consider the concentrated regime and show how the pulling force can vanish at a sufficiently low tension. We show furthermore how this critical tension depends on the protein density on the vesicle.

Free energy. The membrane free energy that we use consists of the Helfrich bending energy and energies that account for protein mixing entropy and protein–protein interactions. We consider the system consisting of a GUV, a tongue aspirated in a pipette, and a long membrane tube, as shown in Fig. S5.

The free energy of this system is written as

$$F = F_p + F_v + F_t - PV_{\rm tot} + \sigma A_{\rm tot} - \mu N_{\rm tot}, \qquad \textbf{[S8]}$$

where F_p, F_v, and F_p are the free energies of the pipette-aspirated tongue, the vesicle, and the tube. The quantities P, σ, μ are Lagrange multipliers introduced to keep the total volume, $V_{\rm tot}$, the total area, $A_{\rm tot}$, and the total number of proteins, $N_{\rm tot}$, constant. The total volume of the system is

$$V_{\rm tot} = V_p + V_v + V_t, \qquad \textbf{[S9]}$$

where

$$V_p = \pi R_p^2 L_p, \qquad \textbf{[S10]}$$

$$V_v = \frac{4}{3}\pi R_v^3, \qquad \textbf{[S11]}$$

$$V_t = \pi R_t^2 L_t, \qquad \textbf{[S12]}$$

and where R_p is the pipette radius, L_p is the tongue length, R_v is the vesicle radius, R_t is the tube radius, and L_t is the tube length. The total area of the system is

$$A_{\rm tot} = A_p + A_v + A_t, \qquad \textbf{[S13]}$$

where

$$A_p = 2\pi R_p L_p, \qquad \textbf{[S14]}$$

$$A_v = 4\pi R_v^2 - \pi R_p^2, \qquad \textbf{[S15]}$$

$$A_t = 2\pi R_t L_t. \qquad \textbf{[S16]}$$

We note that we have neglected the extremities of the tongue and the tube. In fact, when we minimize the free energy with respect to L_p and L_t, these constant terms vanish, and hence are not important here. Finally, the total protein number is

$$N_{\rm tot} = \rho(\phi_p A_p + \phi_v A_v + \phi_t A_t), \qquad \textbf{[S17]}$$

where ϕ_p, ϕ_v, and ϕ_t are the protein area fractions on the tongue, vesicle, and tube. The constraint on the protein number is an approximation. In effect, in the dilute regime, we assume that the adsorption of proteins from the bulk solution is a much slower process than diffusion between the tube and vesicle. In the concentrated regime, we assume that all available charged receptor lipids are saturated, so that no new adsorption occurs over the time scale of the experiment; see *Langmuir isotherm*.

In the dilute regime, we neglect interactions between proteins and the effect of binding of individual proteins to the membrane is modeled by a concentration-dependent spontaneous curvature. We assume that the concentration of proteins on the pipette and vesicle is always low enough so that protein–protein interactions there may be neglected. In this regime, the individual energies of the pipette tongue, vesicle, and tube are

$$F_p = P_p V_p + A_p\left\{\frac{\kappa}{2}\left[\frac{1}{R_p} - C_0(\phi_p)\right]^2 + f_m(\phi_p)\right\}, \qquad \textbf{[S18]}$$

$$F_v = P_0 V_v + A_v\left\{\frac{\kappa}{2}\left[\frac{2}{R_v} - C_0(\phi_v)\right]^2 + f_m(\phi_v)\right\}, \qquad \textbf{[S19]}$$

$$F_t = P_0 V_t + A_t\left\{\frac{\kappa}{2}\left[\frac{1}{R_t} - C_0(\phi_t)\right]^2 + f_m(\phi_t)\right\} - fL_t. \qquad \textbf{[S20]}$$

First, in Eq. **S18**, P_p is the pressure in the pipette, $C_0(\phi)$ is the protein area fraction-dependent spontaneous curvature, and $f_m(\phi)$ is the mixing free energy, given by

$$f_m(\phi) = k_{\rm B}T\rho[\phi\ln\phi + (1-\phi)\ln(1-\phi)], \qquad \textbf{[S21]}$$

where $k_{\rm B}$ is Boltzmann's constant and ρ is the inverse area per protein. Second, in Eq. **S19**, P_0 is the pressure outside the vesicle. Finally, in Eq. **S20**, f is the force exerted on the free end of the tube. In the concentrated regime, the only change to the above is the form of the tube free energy. In this regime, we assume that a dense, scaffold-like structure of proteins forms around the tube, imposing a particular radius, R_a. The tube free energy is then given by

$$F_t = P_0 V_t + A_t[W(\phi_t) + f_m(\phi_t)] - fL_t, \qquad \textbf{[S22]}$$

where $W(\phi_t)$ is the enthalpy density, which includes membrane bending and protein–protein interactions. The protein fraction ϕ_t is assumed to be fixed in the concentrated regime by the protein–protein interactions existing within the scaffold.

Protein binding in the dilute regime. To determine the protein sorting, tube radius, and force in the dilute regime, we treat the pipette and vesicle as flat membrane surfaces: $1/R_p = 1/R_v = 0$. Next, following refs. 10 and 11, we assume that the spontaneous curvature is a linear function of protein area fraction:

$$C_0(\phi) = \tilde{C}_0\phi, \qquad \textbf{[S23]}$$

where $\tilde{C}_0$ is the effective spontaneous curvature; see main text. Making these assumptions and minimizing F with respect to ϕ_p and ϕ_v, we find $\phi_p = \phi_v$ and

$$\rho\mu = f_m'(\phi_v) + \kappa\tilde{C}_0^2\phi_v, \qquad \textbf{[S24]}$$

where f_m' denotes a derivative of f_m with respect to ϕ. Minimization of F with respect to L_p and R_v then yields the Laplace law

$$P_0 - P_p = \frac{2\tilde{\sigma}}{R_p}\left(1 - \frac{R_p}{R_v}\right), \qquad \textbf{[S25]}$$

where

$$\tilde{\sigma} = \sigma + \frac{\kappa\tilde{C}_0^2\phi_v^2}{2} + f_m(\phi_v) - \rho\mu\phi_v = \sigma - \frac{\kappa\tilde{C}_0^2\phi_v^2}{2} + k_{\rm B}T\rho\ln(1-\phi_v) \qquad \textbf{[S26]}$$

is the physically controlled membrane tension. We may then write the effective tube free energy $F_t' = F_t - \rho\mu\phi_t A_t + \sigma A_t$ and expand it to second order in $\Delta\phi \equiv \phi_t - \phi_v$, obtaining

$$F_t' = 2\pi R_t L_t\left[\frac{\kappa}{2}\left(\frac{1}{R_t^2} - \frac{2\tilde{C}_0\phi_t}{R_t}\right) + \tilde{\sigma} + \frac{1}{2}\chi\Delta\phi^2\right] - fL_t, \qquad \textbf{[S27]}$$

where $\chi = f''_m(\phi_v) + \kappa\bar{C}_0^2$ is the effective osmotic susceptibility. Because the protein density on the vesicle is assumed to be always small, in the main text we use the $\phi_v = 0$ limit of χ, namely $\chi = k_B T\rho/\phi_v + \kappa\bar{C}_0^2$. We note that we have neglected the $(P_0 - P)V_t$ term in Eq. **S27** because it is of order R_t/R_v smaller than the other terms.

We now calculate ϕ_t, R_t, and f. Minimizing Eq. **S27** with respect to ϕ_t yields

$$\Delta\phi = \frac{\kappa\bar{C}_0}{\chi R_t}, \qquad \textbf{[S28]}$$

which is a linear function of the tube curvature. Next, minimizing Eq. **S27** with respect to R_t yields the tube radius

$$R_t = \sqrt{\frac{\kappa_{\text{eff}}}{2\tilde{\sigma}}}, \qquad \textbf{[S29]}$$

where $\kappa_{\text{eff}} = \kappa(1 - \kappa\bar{C}_0^2/\chi)$ is the renormalized bending modulus. Finally, minimizing F'_t with respect to L_t gives the force

$$f = 2\pi\sqrt{2\kappa_{\text{eff}}\tilde{\sigma}} - 2\pi\kappa\bar{C}_0\phi_v. \qquad \textbf{[S30]}$$

We see that the tube radius and tube force scale with tension in the same way in the dilute regime as in the absence of proteins.

Protein binding in the concentrated regime. We next consider the mechanical effects of protein binding on the membrane tube in the concentrated regime. It is assumed that, in this regime, all charged receptor lipids are bound to proteins. As before, the tube force is obtained by minimizing the effective tube free energy $F'_t = F_t + \sigma A_t - \rho\mu\phi_t A_t$, with respect to L_t, but now F_t is given by Eq. **S22**. The protein density on the tube, ϕ_t, is fixed, yet because of protein number and membrane area conservation, as the tube length is varied, the density ϕ_v will vary. This effect is captured here by introducing the Lagrange multiplier μ. Performing $\partial F'_t/\partial L_t = 0$, and using Eqs. **S24** and **S26**, we obtain

$$\begin{aligned} f &= 2\pi R_a\left\{\tilde{\sigma} + W(\phi_t) + \kappa\bar{C}_0^2\phi_v\left(\frac{\phi_v}{2} - \phi_t\right)\right. \\ &\quad \left. + k_B T\rho\left[\phi_t \ln\left(\frac{\phi_t/(1-\phi_t)}{\phi_v/(1-\phi_v)}\right) + \ln\left(\frac{1-\phi_t}{1-\phi_v}\right)\right]\right\} \\ &= 2\pi R_a(\tilde{\sigma} - \sigma^*), \end{aligned} \qquad \textbf{[S31]}$$

where σ^* is the tension at which the pulling force vanishes, given by

$$\begin{aligned} \sigma^* &= -W(\phi_t) - \kappa\bar{C}_0^2\phi_v\left(\frac{\phi_v}{2} - \phi_t\right) \\ &\quad + k_B T\rho\left[\phi_t \ln\left(\frac{\phi_v/(1-\phi_v)}{\phi_t/(1-\phi_t)}\right) + \ln\left(\frac{1-\phi_v}{1-\phi_t}\right)\right]. \end{aligned} \qquad \textbf{[S32]}$$

For $\phi_t \gg \phi_v$ and $\phi_v, \phi_t \ll 1$ this expression simplifies to

$$\sigma^* = -W(\phi_t) + \kappa\bar{C}_0^2\phi_t\phi_v + k_B T\rho\phi_t \ln\left(\frac{\phi_v}{\phi_t}\right). \qquad \textbf{[S33]}$$

We note the dependence of σ^* on ϕ_v: As shown in the main text, the linear term, $\kappa\bar{C}_0^2\phi_t\phi_v$, when fitted to the experimental results, allows a determination of the intrinsic curvature $\bar{C}_0$.

1. Angelova M, Soléau S, Méléard P, Faucon JF, Bothorel P (1992) Preparation of giant vesicles by external ac electric fields. kinetics and applications. *Prog Colloid Polym Sci* 89:127–131.
2. Mathivet L, Cribier S, Devaux PF (1996) Shape change and physical properties of giant phospholipid vesicles prepared in the presence of an AC electric field. *Biophys J* 70:1112–1121.
3. Carvalho K, Ramos L, Roy C, Picart C (2008) Giant unilamellar vesicles containing phosphatidylinositol(4,5)bisphosphate: Characterization and functionality. *Biophys J* 95:4348–4360.
4. Roux A, Uyhazi K, Frost A, De Camilli P (2006) Gtp-dependent twisting of dynamin implicates constriction and tension in membrane fission. *Nature* 441:528–531.
5. Sorre B, et al. (2009) Curvature-driven lipid sorting needs proximity to a demixing point and is aided by proteins. *Proc Natl Acad Sci USA* 106:5622–5626.
6. Ambroggio E, et al. (2010) Arfgap1 generates an arf1 gradient on continuous lipid membranes displaying flat and curved regions. *EMBO J* 6:292–303.
7. Derenyi I, Julicher F, Prost J (2002) Formation and interaction of membrane tubes. *Phys Rev Lett* 88:238101.
8. Galush WJ, Nye JA, Groves JT (2008) Quantitative fluorescence microscopy using supported lipid bilayer standards. *Biophys J* 95:2512–2519.
9. Bhatia VK, et al. (2009) Amphipathic motifs in bar domains are essential for membrane curvature sensing. *EMBO J* 28:3303–3314.
10. Marcerou JP, Prost J, Gruler H (1984) Elastic model of protein–protein interaction. *Nuovo Cimento Soc Ital Fis D* 3:204–210.
11. Campelo F, McMahon HT, Kozlov MM (2008) The hydrophobic insertion mechanism of membrane curvature generation by proteins. *Biophys J* 95:2325–2339.

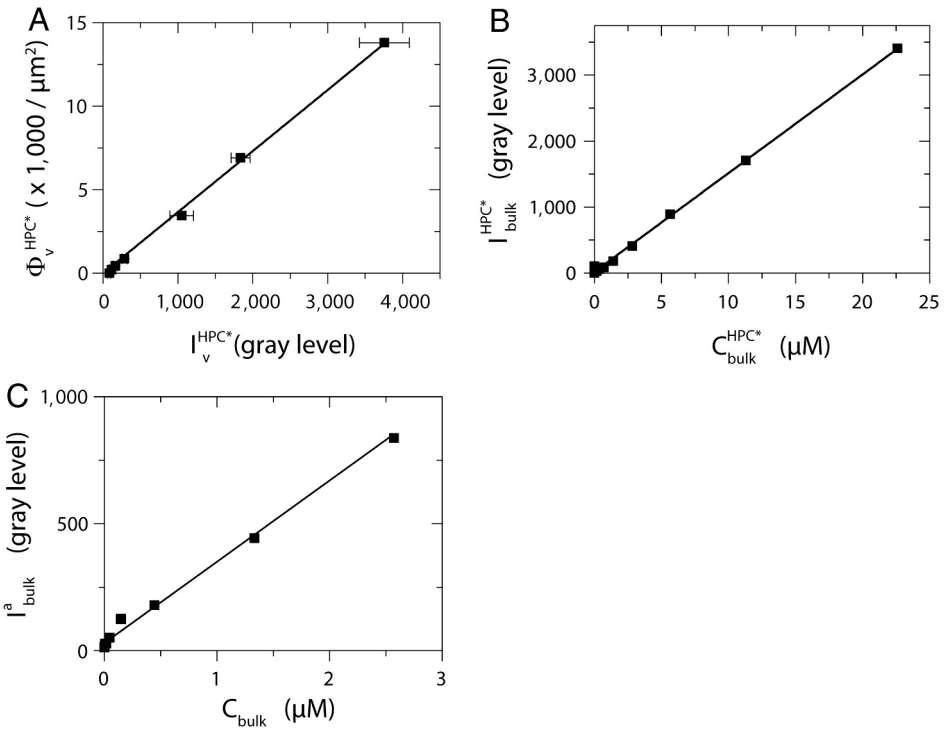

Fig. S1. Fluorescence calibration. (*A*) Fluorescence measured with confocal in the green channel, $I_v^{HPC^*}$, from GUVs membrane containing increasing amount of HPC*, $\Phi_v^{HPC^*}$, expressed in number of molecules per micron squared. Linear fit $\Phi_v^{HPC^*} = A^{gain} \times I_v^{HPC^*}$ gives the conversion constant, $A^{gain} = 3.8 \pm 0.1$, (six GUVs) in these acquisition conditions. (*B*) Fluorescence measured in bulk ($I_{bulk}^{HPC^*}$) using SUVs, as a function of the volume concentration of HPC* ($C_{bulk}^{HPC^*}$). Linear fit to $I_{bulk}^{HPC^*} = a^{HPC^*} \times C_{bulk}^{HPC^*}$ gives a^{HPC^*} 150 ± 2. (*C*) Amph1* fluorescence signal (I_{bulk}^{a}) measured in bulk using SUVs, as a function of the volume concentration of amph1* (C_{bulk}). Linear fit to $I_{bulk}^{a} = a^{amph1^*} \times C_{bulk}$ gives $a^{amph1^*} = 280 \pm 10$. The efficiency ratio F_1 is defined as $F_1 = \frac{a^{amph1^*}}{a^{HPC^*}} = 1.8 \pm 0.1$. All the data presented in this figure were acquired using the same excitation/acquisition conditions.

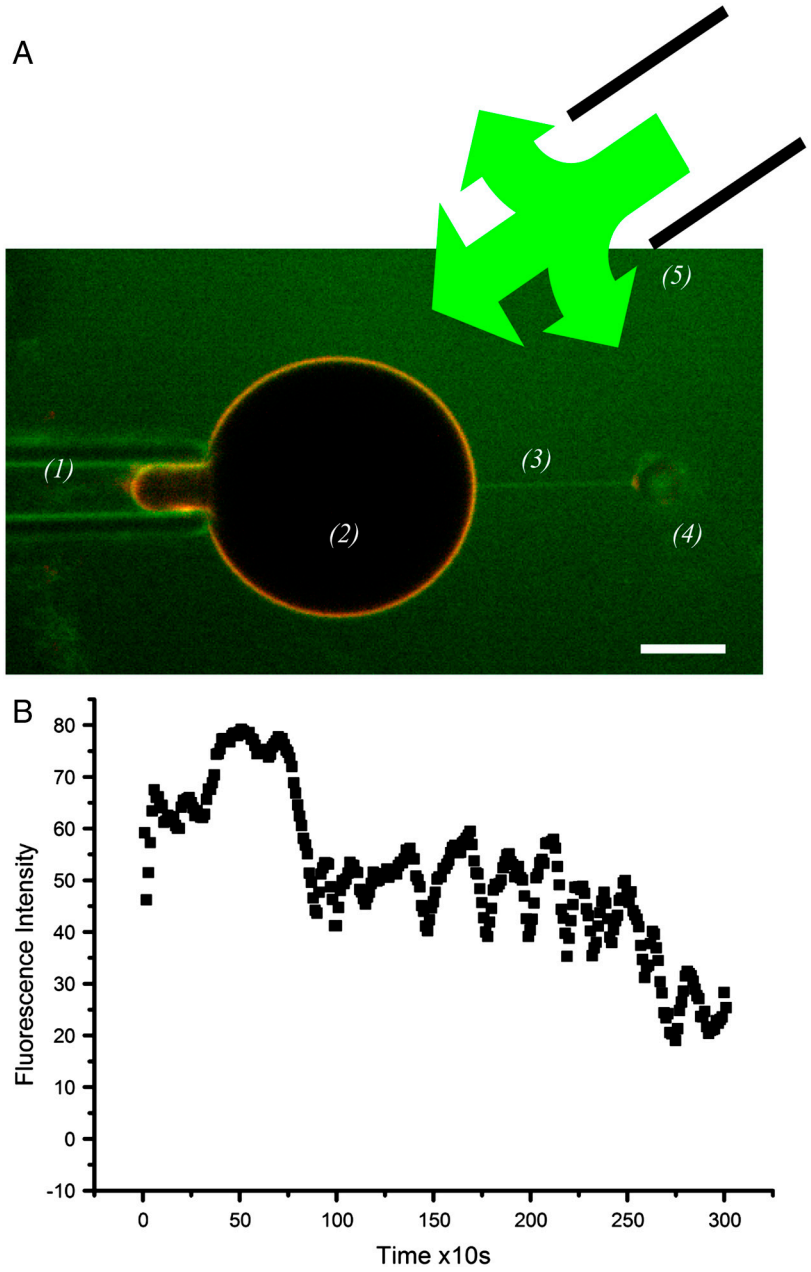

Fig. S2. (*A*). Confocal image of experimental setup with schematic illustration of the protein solution injection. (Scale bar: 5 μm.) (*1*) Aspiration pipette holding the GUV and used to set membrane tension. (*2*) GUV. (*3*) Tube pulled from the GUV. (*4*) Polystyrene bead held in an optical trap that is used to pull the tube and to measure the tube pulling force. (*5*) Pipette used to inject labeled amphiphysin; direction of flow is indicated by arrows (roughly to scale). (*B*) Absence of desorption of amph1*. A single GUV aspirated in a micropipette is flushed with a second pipette containing a solution of 2.5 μM amph1* for 750 s (0–750 s on the graph). The second pipette is then removed (approximately 750 s on the graph). The fluorescence intensity was obtained from the maximum of the fluorescence profile over a cross-section passing across the vesicle, with an averaging window of three images (one image every 1.5 s). The fluorescence of the protein stays roughly constant during 2,000 s, indicating very slow desorption of amph1*.

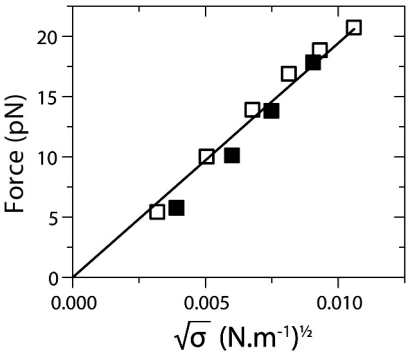

Fig. S3. Control experiment: Comparison of the force as a function of $\sqrt{\sigma}$ between experiments in the presence of an injected solution containing buffer but no protein (■) and in the absence of injection (□). Linear fit according to $f = 2\pi\sqrt{2\kappa\sigma}$ gives $f = 1{,}900 \pm 100 \times \sqrt{\sigma}$; $(\kappa = 11 \pm 1\ k_B T)$.

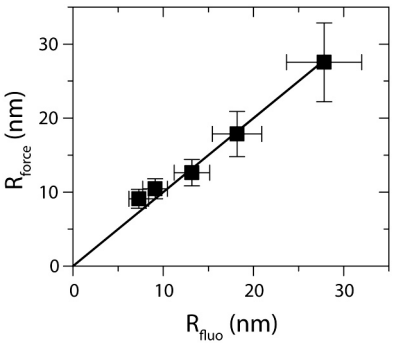

Fig. S4. Comparison of the tube radius measurements deduced from the force and from the calibrated fluorescence signal, in the absence of proteins in solution. R_{force} was deduced from Eq. **S1**: $R_{\text{force}} = \frac{\kappa}{4\pi\sigma}$. R_{fluo} was measured using the calibrated fluorescence ratio $(\frac{I_{\text{tube}}}{I_{\text{GUV}}})$ of lipid dyes in the membrane $R_{\text{fluo}} = 200 \pm 50 \times \frac{I_{\text{tube}}}{I_{\text{GUV}}}$. The calibration prefactor was measured using six independent experiments. Line: $R_{\text{force}} = R_{\text{fluo}}$.

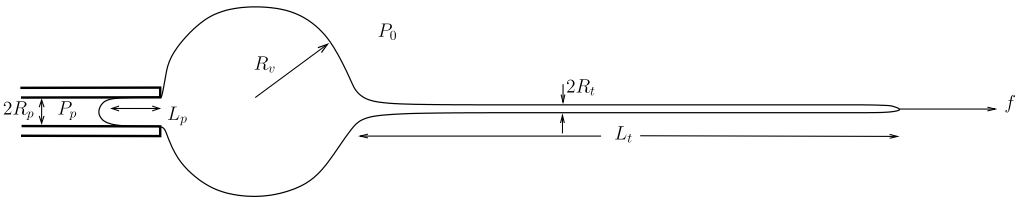

Fig. S5. Schematic of the system as used in the theoretical part.

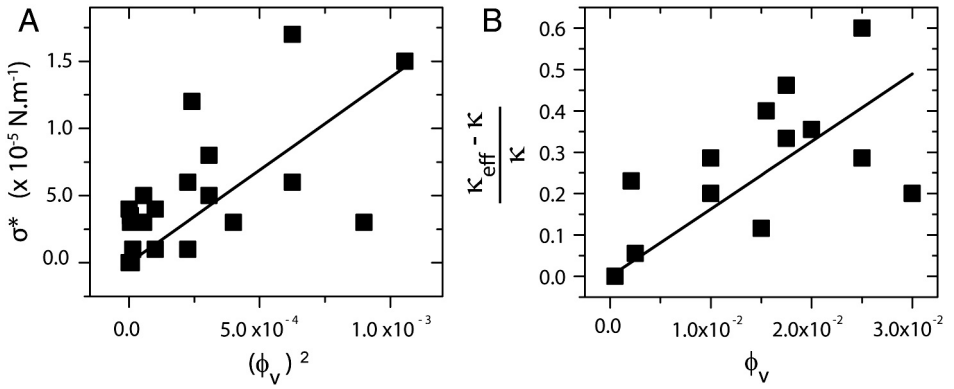

Fig. S6. Intermediate regime. (*A*) Plot of σ^* as a function of the squared protein area fraction on the vesicle, ϕ_v, in the intermediate density regime. The tension at which the force, f, vanishes is σ^*. Data are fitted to $\sigma^* = (14 \pm 5) \times 10^{-3}\phi_v^2$ N/m. (*B*) Effective bending rigidity as of the protein area fraction on the vesicle, ϕ_v. Data are fitted to $(\kappa - \kappa_{\text{eff}})/\kappa = 15 \pm 5\phi_v$.

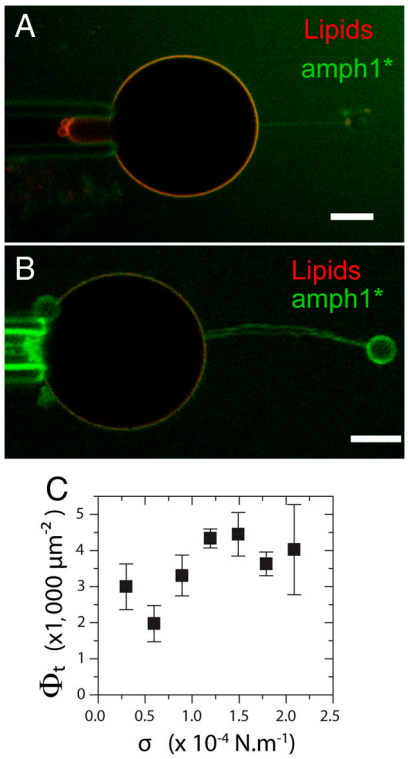

Fig. S7. Confocal fluorescence image of a tube pulling experiment in the high-density regime (*A*) Image corresponding to experiment presented in Fig. 4. Note the homogeneous distribution of protein on the tube. Membrane is labeled using a red lipid dye (BODIPY TR ceramide, red fluorescence channel) and amphiphysin 1 (amph1*, green channel) is labeled with Alexa 488. In this experiment, $\Phi_v = 1{,}100 \pm 100\ \mu m^{-2}$. (Scale bar: 5 μm.) (*B*) Stabilization of the tube by amph1* in the high-density regime. At high Φ_v, the tube no longer retracts when optical tweezers are turned off. Confocal fluorescence picture: The membrane is labeled using a red lipid dye (BODIPY TR ceramide, red fluorescence channel) and amphiphysin 1 (amph1*, green channel) is labeled with Alexa 488. Tube appears blurry due to movements between averaged frame acquisitions. (Scale bar: 5 μm.) (*C*) Protein density on the tube (Φ_t) versus membrane tension (σ) for the vesicle presented in Fig. 4.

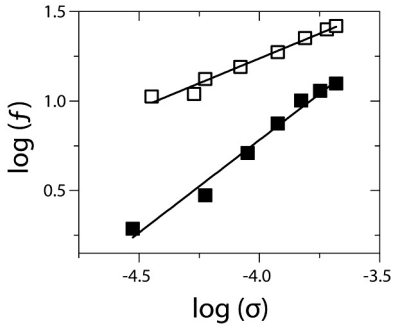

Fig. S8. Effect of protein binding in the high-density regime. Log–log plot of the force versus tension corresponding to Fig. 4*A*. It shows the change in scaling of the force with tension upon protein binding in the high-density regime. Linear fit to data taken in the absence of protein in solution (□) gives $\log(f) = (0.55 \pm 0.03) \times \log(\sigma) + (3.5 \pm 0.1)$, whereas when amphiphysin is in solution (■) the fit yields $\log(f) = (1.03 \pm 0.06) \times \log(\sigma) + (4.9 \pm 0.2)$.

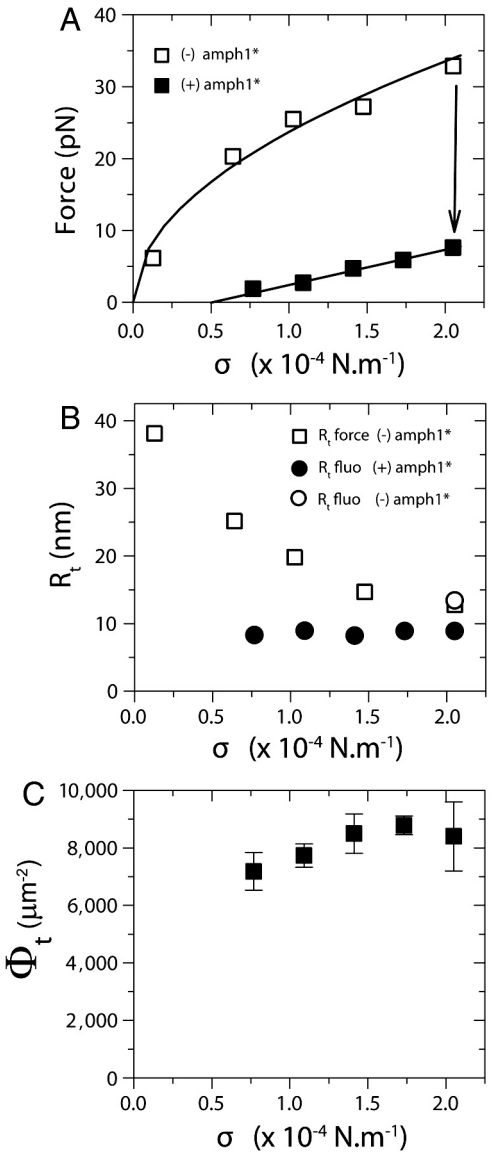

Fig. S9. Another example of vesicle in the high Φ_v regime. The experiments presented in this figure correspond to a single GUV with $\Phi_v = 2{,}100 \pm 500\ \mu m^{-2}$. (*A*) Effect on the tube force of the presence of amphiphysin 1 in solution. The force in the presence of amph1* bound to the membrane (■) is lowered as compared to in its absence (□). Following Fig. S5*B*, data in the absence of protein are fitted to $\sqrt{\sigma}$: $f = 2370 \times \sqrt{\sigma}$; ($\kappa \approx 17\ k_BT$), whereas when amph1* is bound, a linear variation between the force and σ is measured together with a shift of the origin of the force to nonzero tension. Fit $f = (4.9 \times 10^{-4}) \times \sigma - 2.5$; $\sigma^* = 5 \times 10^{-5}$ N · m^{-1}. (*B*) Effect on the tube radius of the presence of amph1* in solution; tube radius R_t versus membrane tension σ in the absence (empty symbols, deduced from force or fluorescence) or with amph1* (full symbols deduced from fluorescence) in solution. (*C*) Variation of amph1* density on the tube Φ_t with membrane tension. Error bars based on standard deviation on four measurements.

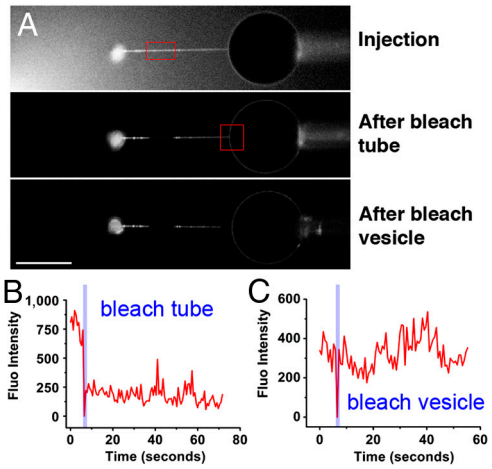

Fig. S10. Fluorescence recovery after photobleaching (FRAP) experiment on amph1*-coated tube and GUV. (*A*) Images taken during amph1* injection (at 0 s) then again at 2 min, 30 s after injection [approximately 1 min, 30 s after bleaching of the tube (bleached area corresponds to the red box in the 0 s image)], and approximately 5 min after injection, corresponding to 1 min, 30 s after bleach of the vesicle (bleach area corresponds to the red box in the 2 min, 30 s image). On this last image, no recovery is observed on the tube. (*B*) Fluorescence intensity along the tube in the box shown in the 0 s image in *A*) (the bleach time corresponds to the vertical blue line). (*C*) Fluorescence intensity along the portion of the vesicle in the red box shown in the 2 min, 30 s image in *A*). (Scale bar: 10 μm.)

Table S1. Summary of data in the high-density regime

Φ_v, μm^{-2}	σ^*, $\times 10^{-5}$ N·m^{-1}	Φ_t, μm^{-2}	R_t, nm
2,100 ± 500	5 ± 2.5	8,100 ± 650	6
1,400 ± 300	1.5 ± 0.3	7,500 ± 650	5
1,100 ± 200	1 ± 0.9	3,500 ± 850	6
1,800 ± 250	4.6 ± 2	3,200 ± 750	4
800 ± 200	0.5 ± 0.6	4,900 ± 2000	10
1,450 ± 250	4.7 ± 2	2,700 ± 150	6
900 ± 150	0.8 ± 0.8	4,200 ± 300	12

For each experiment, Φ_v is the amph1* density on the GUV, σ^* is the tension at which the measured force vanishes (see Fig. 3 and Fig. S7), Φ_t is the amph1* density measured on the tube, and R_t the value of the tube radius at $\sigma = 2 \times 10^{-5}$ N · m^{-1}